International Journal of Recent Technology and Engineering (IJRTE)
ISSN: 2277-3878 (Online), Volume-8 Issue-2, July 2019

Numerical Analysis of Protrusion Effect over an Airfoil at Reynolds Number -10^5

Aslesha Bodavula, Ugur Guven, Rajesh Yadav

Abstract*: Need of micro aerial vehicles and Unmanned Air Vehicles is increasing due to military, defense and civilian requirements. These vehicles fly at very small Reynolds numbers and have to move in confined spaces with a bare minimum speed, to achieve high lift coefficient is the main concern. The main focus of this research paper is to carry out the computational analysis and study the unsteady flow over NACA0012 airfoil with right angle triangular protrusion at the Reynolds number 10^5. The location of the protrusion is 0.05c, with three different heights of protrusion 0.005c, 0.01c, and 0.02c, normal to the surface of the airfoil. Geometric modeling and grid generation are created using the ICEM CFD software and numerical analysis carried out using CFD Software at various angle of attacks ranging from 0^0 to 16^0 with 2^0 intervals. Numerical validation has done and compared. The results obtained from the research work is recommend that for smaller protrusions the lift and drag coefficients are unaffected in the low angle of attacks while the lift characteristic is significantly improved at the higher angle of attacks.

***Index Terms*: Low Reynolds number, NACA 0012, Vortex Shedding, MAVs, UAVs, Wind Energy.**

I. INTRODUCTION

Low Reynolds number flows are turn out to be the main concern area of so many researchers due to progress and usage of the Micro Aerial Vehicles (MAV), Unmanned Aerial Vehicles (UAV), helicopters, sailplanes and high altitude vehicles. These MAV's, UAV's are used mostly in military, defense and civilian sectors [1]. These aerial vehicles are also used for traffic control, monitoring the pipelines in chemical industries, wildlife photography and to rescue wild animals or people from danger. Recently, research on the UAV's and MAV's at the mars exploration mission are exploring by the researchers [2]. The atmospheric properties of the mars are low density and temperature affects the low Reynolds number aerodynamics which plays a crucial role in designing the micro aerial vehicles at Martian atmosphere [2]. Size of micro aerial vehicles varies from small size to large size; the typical ranges are 0.1- 0.5 meters and fly at very low altitude and Reynolds number [1].

Another application area of the Low Reynolds number flow is wind turbines used to extract the wind energy. It is one of the renewable energy resources. It is used to avoid the burning of the fossil fuels releases the gases into the earth's atmosphere and creates the global warming in the environment. When these fossil fuels burnt, so many pollutants are discharge to the air, soil and water. These pollutants have the impact on earth's atmosphere. To overcome come from this air pollution and toxic gases, can use the renewable energy. It is trending that renewable energy source is to avoid global warming occurring due to chemical industries and fuel based power plants. Renewable energy uses the nature sources like wind, solar, hydro, biomass, biofuels and geothermal. This research is inclined towards the wind energy. Wind energy haul out with the help of wind turbines.

Apart from conventional wind turbines, renewable energy from wind kinetic energy can be extracted through wing-mills [3], [4], kites [5], [6] mechanisms based on Vortex Induced Vibrations [7] –[10]. All these energy extraction mechanisms use some form of movement of wings, flat plate or cylindrical objects through application of aerodynamic forces at low Reynolds number.

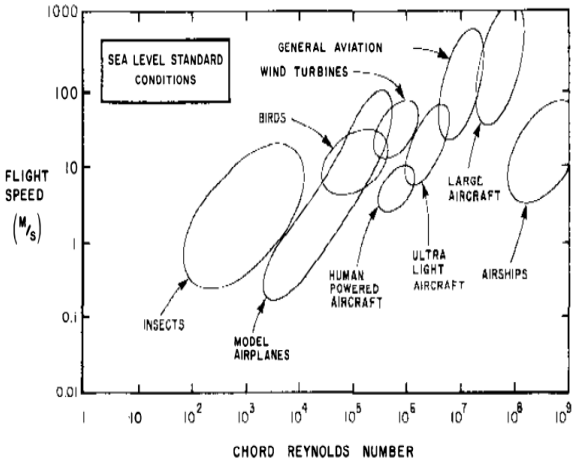

Fig.1: Flight Speed versus Chord Reynolds number [1]

MAVs, UAVs and also energy harvesters at Low Reynolds number, functional in the range of 10^4 to 10^7 is very interesting and involves complex unsteady flow phenomena [1], [11]. At this flow regime, can observe the separation of the flow on the suction surface of the airfoil due to adverse pressure gradient, transition and reattachment. One of the strange behaviors of airfoil at low Reynolds number is vortex shedding. From the reference [12], it was found that the cause of vortex shedding is due to intervening inviscid instability wave prompted by the inflection velocity profile downstream of the separation point.

Revised Manuscript Received on 30 July 2019.
***** Correspondence Author
Aslesha Bodavula*, Department of Aerospace Engineering, University of Petroleum and Energy Studies, Dehradun, INDIA.
Ugur GUVEN, Department of Aerospace Engineering, University of Petroleum and Energy Studies, Dehradun, INDIA
Rajesh Yadav, Department of Aerospace Engineering, University of Petroleum and Energy Studies, Dehradun, INDIA

Vortex shedding is also exaggerated by the angle of attack with greater angle of attack accounting for elongated the vortex shedding sequences [13]. At low Reynolds number, the development of laminar separation bubble take place on the upper and lower surface of the airfoil at small angle of attack [13]. Experimental study of NACA 0025 done by [14], performance over the airfoil diminishes steadily due to the failure of reattachment of separated shear layer on airfoil surface at the Reynolds number 100000. At chord Reynolds number 150000, the separated shear layer experiences transition and reattaches to the NACA 0025 airfoil surface [14]. This deprivation in performance is again caused by the failure of the shear layer to reattach. A detailed numerical work [15] done to appreciate the aerodynamics performance of numerous airfoils at low Reynolds numbers.

In real time scenario these low Reynolds number vehicles are subject to surface roughness of many forms, size and source. At low Reynolds number, the flow is highly subjected to surface characteristics and hereafter these protrusions can modify the aerodynamics of these wings extensively. Experimental work conducted on the distributed leading edge roughness over an airfoil at different Reynolds number range, from the results it was found as the Reynolds number increasing from low to high the performance of the aerodynamics over an distributed leading edge roughness is mortifying [16]. The characteristics of separation bubble behind protrusion affected by icing and its influence on flow instability. They revealed that increasing the angle of attack for NLF-0414 airfoil lead to in extended separation bubbles at modest Reynolds numbers. They also conveyed a fall in vortex shedding frequency as the incidence was greater than before [17].

Some bio-inspired wings, with sinusoidal leading edge protuberance named tubercles may increase the aerodynamic efficiency of wings and wind turbines. These sinusoidal protrusions at the leading edge are favorable only in the post stall regime, for conventional NACA 4-digit airfoils [18]. The improvements in post stall aerodynamic characteristics and stalling angle progress more with increasing Reynolds number in the range 75000-300000 [19].

In spite of that there is a necessity to explore about the pioneering passive flow control devices that can markedly enrich the performance of the Wind turbines and MAVs. At low Reynolds number, even the small change or irregularities of the airfoil shape can change the aerodynamic characteristics extensively based on size, shape and location of the protrusions on wing surface. The effect these protrusions are also dependent on the thickness, location of maximum thickness and the angle attack of the configuration. The main objective of this paper is to inspect the effect of size of a right angle triangular protrusion located at the 0.5%chord on the suction surface (upper surface of the airfoil) with three different heights of protrusion that is 0.5%chord, 1%chord, 2%chord respectively. The Reynolds number of the flow is considered to be 100000. Numerical analysis over an airfoil with protrusion is carried out at various angle of attacks (AOA) ranging from 0^0 to 16^0 with 2^0 intervals using the CFD Software ANSYS FLUENT®.

II. NUMERICAL METHODOLOGY

A. Geometric Modeling and Grid Generation

NACA0012 airfoil has chosen for conducting the numerical simulation. Geometry and grid generation of the NACA0012 airfoil with and without protrusions on the surface of the airfoil generated with the ICEMCFD® as shown in Fig. 2. The chord length of the airfoil in each case is 0.1m and protrusions are located at 0.05c on the surface of the airfoil. Protrusion at this location on suction surface has the three different heights of 0.005c, 0.01c, and 0.02c. To study the flow effects around the airfoil a C-shaped domain with multi-block structured meshes created using ICEMCFD®, as shown in Fig. 3. The C-topology computational domain extends to 20 times the chord length in all directions, from the airfoil. The first cell distance from the surface of the airfoil in each case is set to 0.000019m to have a non-dimensional cell wall distance $y+ \approx 1$.

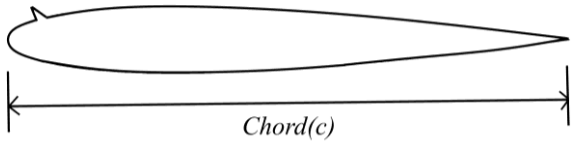

Fig. 2: NACA0012 airfoil with Protrusion at 0.05c

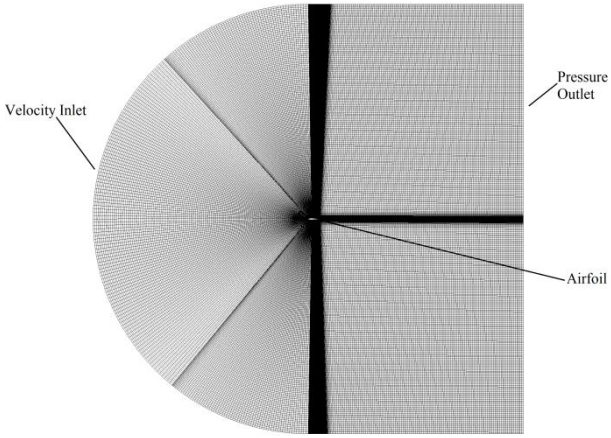

Fig. 3: Grid around NACA 0012 with protrusion on suction surface

B. Governing equations and solver

To analyze the flow over an airfoil a two-dimensional unsteady Navier-Stokes equations, given by Eqns. (1) and (2) are solved using finite volume solver ANSYS FLUENT®. The continuity equation and the two momentum equations are solved in a segregated manner using a pressure based algorithm. The coupling of pressure and velocity fields is attained through SIMPLE scheme, which is based on predictor-corrector approach to enforce mass conservation.

$$\frac{\partial \rho}{\partial t} + \nabla.\left(\rho \vec{V}\right) = 0 \qquad (1)$$

$$\frac{\partial}{\partial t}(\rho\vec{V}) + \nabla.(\rho\vec{V}\vec{V}) = -p\delta_{ij} + \tau_{ij} \quad (2)$$

where δ_{ij} is the kronecker delta and the viscous stress tensor τ_{ij} in Eq. 2, is given by

$$\tau_{ij} = \mu\left[\left(\frac{\partial u_i}{\partial x_j} + \frac{\partial u_j}{\partial x_i}\right) - \frac{2}{3}\delta_{ij}\frac{\partial u_k}{\partial x_k}\right]$$

All the conservation equations are discretized using a second order upwind scheme with higher order under-relaxation factor of 0.75 applied to all flow variables. Second order accurate implicit transient formulation. Starting the simulation with steady state solutions as first guess, the equations are solved iteratively at each time step before going forward to the next time step, with a static time step of 1e-04 seconds.

C. Turbulence Modeling

The turbulence model thus, selected here is a 4-equation transition model viz. Transition SST model [20]. This model is based on the correlation based coupling of the two-equation SST k-ω model [21] with two extra equations for the transport of intermittency (γ) and transition-onset momentum-thickness Reynolds number ($Re_{\theta t}$).

$$\frac{\partial(\rho k)}{\partial t} + \frac{\partial(\rho U_j k)}{\partial x_j} = \widetilde{P_k} - \beta^*\rho k\omega + \frac{\partial}{\partial x_j}\left[(\mu + \sigma_k\mu_t)\frac{\partial k}{\partial x_j}\right] \quad (3)$$

$$\frac{\partial(\rho\omega)}{\partial t} + \frac{\partial(\rho U_j\omega)}{\partial x_j} = \alpha\rho S^2 - \beta\rho\omega^2 + \frac{\partial}{\partial x_j}\left[(\mu + \sigma_\omega\mu_t)\frac{\partial\omega}{\partial x_j}\right] + 2(1-F_1)\rho\sigma_{\omega 2}\frac{1}{\omega}\frac{\partial k}{\partial x_j}\frac{\partial\omega}{\partial x_j} \quad (4)$$

Two extra equations, intermittency and transition-onset momentum thickness Reynolds number given as the following:

$$\frac{\partial(\rho\gamma)}{\partial t} + \frac{\partial(\rho U_j\gamma)}{\partial x_j} = P_\gamma - E_\gamma + \frac{\partial}{\partial x_j}\left[\left(\mu + \frac{\mu_t}{\sigma_\gamma}\right)\frac{\partial\gamma}{\partial x_j}\right] \quad (5)$$

$$\frac{\partial(\rho\widetilde{Re_{\theta t}})}{\partial t} + \frac{\partial(\rho U_j\widetilde{Re_{\theta t}})}{\partial x_j} = P_{\theta t} + \frac{\partial}{\partial x_j}\left[\sigma_{\theta t}(\mu + \mu_t)\frac{\partial\widetilde{Re_{\theta t}}}{\partial x_j}\right] \quad (6)$$

Whereas Eγ is destruction source term, P_γ is source term, $P_{\theta t}$ is production term.

D. Boundary and far-field Conditions

The velocity inlet of the flow is taken based on the Reynolds number and chord length is 15m/s and pressure at outlet of the domain is specified as 1atm. Since the flow is low Reynolds number the turbulent intensity is maintained at 0.1% and Intermittency is 1.

E. Grid Independence Study and Validation

To NACA0012 airfoil, grid independence study is done, to evaluate how many numbers of elements are required for a mesh to independent on the solution. Various mesh elements are considered and carried out the CFD simulations over an NACA0012 clean airfoil at 8^0. To check the grid independence study is achieved or not pressure coefficient values are taken out from the simulation results around the airfoil. Fig. 4 describes about the pressure coefficient around the surface of the airfoil with various mesh counts, from this it was concluded that the pressure coefficient values are same as the number elements are increasing it means that the grid is independent of the solution. Based on this study 169750 elements are considered to carry forward the further numerical analysis and to achieve faster convergence results.

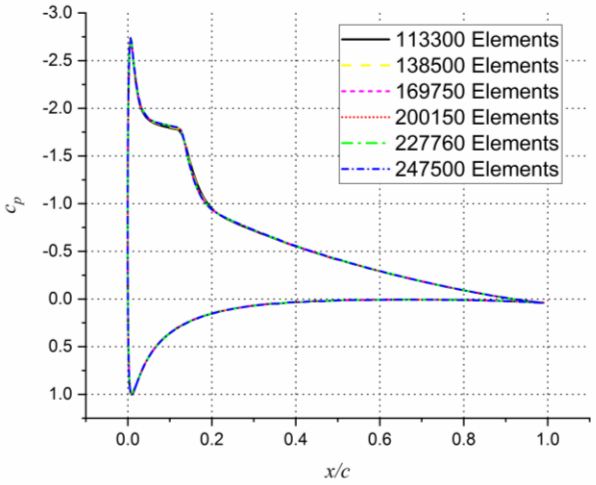

Fig.4: Grid Independence Study

Fig.5, explains about the numerical analysis of the present CFD Study of NACA0012 clean configuration at 8^0, was observed that current numerical analysis data is exhibiting the close agreement with the experimental data [22]. Solver validation is done in counter to the reference [23]. From the validation, it was conclude that the solver setup used for this analysis is perfect to carry out numerical simulation.

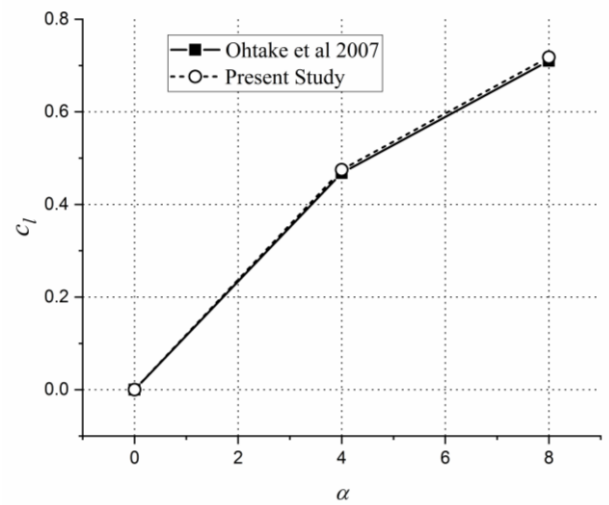

Fig.5: Numerical validation with experimental data [22]

III. Results and Discussion

Numerical Analysis is carried out over an NACA0012 airfoil with right angle triangular protrusion at Reynolds number 100000 at various angles of attack 0^0, 2^0, 4^0, 6^0, 8^0, 10^0, 12^0, 14^0 and 16^0. From the Fig.4, can be seen h=0.005c is exhibiting the same values as clean configuration till 10^0 except in 4^0, 6^0. There is slight drop in lift coefficient values.

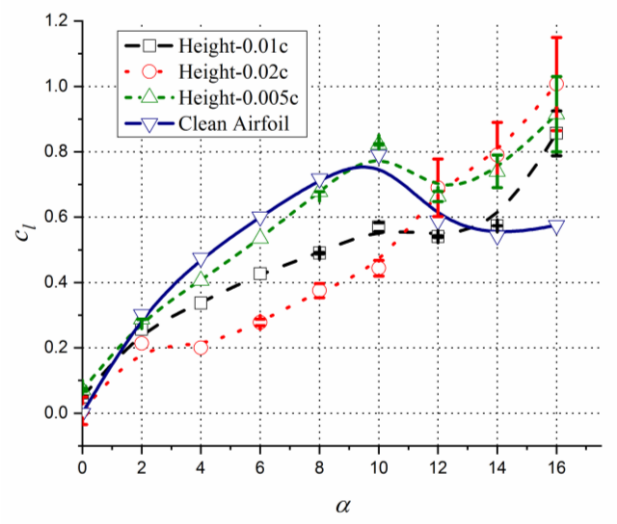

(a) C_l versus α

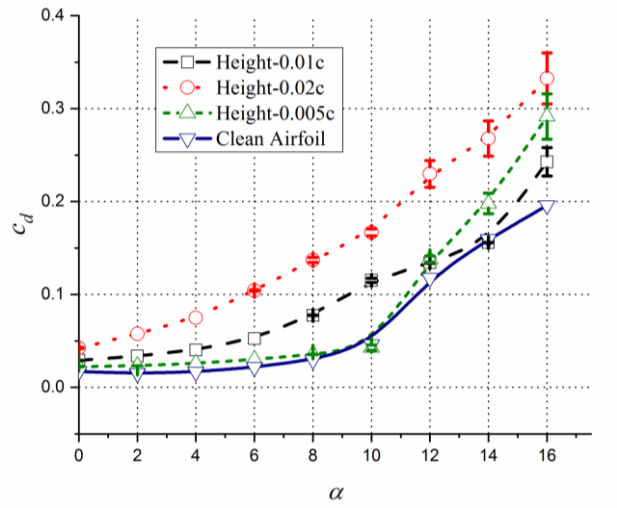

(a) C_d versus α

Fig. 6: Lift and Drag coefficient of Right Angle Triangle protrusion at 0.05c location

Due to adverse pressure gradient, flow is separated from the airfoil at ahead of the protrusion. When the pressure is more than the velocity is less as can see in Fig. 7(b), whereas clean airfoil there is no flow separation near to the leading edge. Aft of the protrusion, it was found the presence of the laminar separation bubble and has been present in the clean configuration as well. Due to flow separation at ahead of the protrusion there is a drop in the lift coefficient.

As the angle of attack rises from 12^0 to 16^0 there is a significant improvement in the lift coefficient observed as can see in Fig. 6(a). This increment is observed due to shedding of vortices from the surface of the airfoil. As the height of the protrusion increases there is a reduction in the lift coefficient observed in low angle of attacks and one more interesting scenario observed is there is no stalling which means there is no drop in the lift coefficient values.

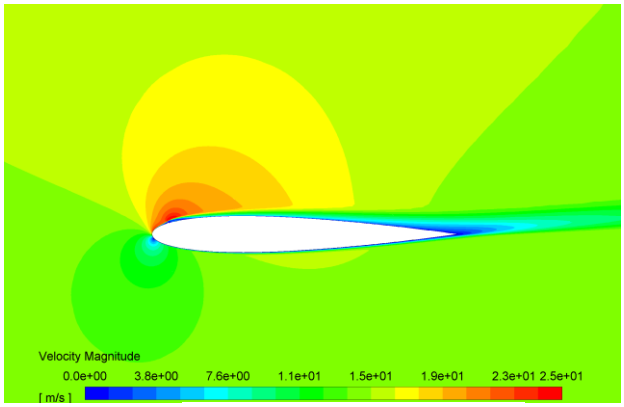

(a) Velocity distribution over an airfoil

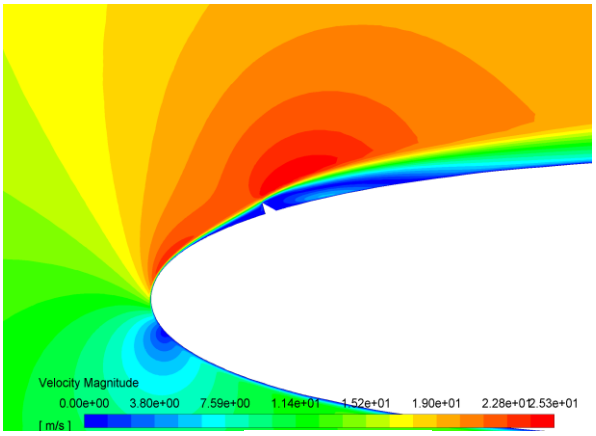

(b) Near the protrusion

Fig. 7: Velocity distribution over an airfoil with protrusion at α= 60

For h=0.01c, 0.02c at angle of attack 6^0, the lift coefficient values are due to the flow separation at ahead of the protrusion and formation of the long laminar separation bubble at aft of the protrusion, because of this there is an reduction in lift coefficient was observed. For h=0.01c, it was observed form 8^0 to 12^0, there is a reduction in the lift coefficient is observed due flow separation phenomenon seen on the entire surface of the airfoil even though there is an vortex formation observed at ahead of the protrusion there is no improvement in the lift coefficient observed. There is increment in the lift coefficient observed at 14^0, 16^0 is due to the effect of the shedding of the vortices. Similar flow phenomenon observed for h=0.02c at 8^0, 10^0. Not only the h=0.02c is exhibited reduction in the lift coefficient but also the increment in the drag coefficient as can see in Fig. 6(b). There is augmentation in the lift coefficient values from 12^0 to 16^0.

Retrieval Number: B2809078219/19©BEIESP
DOI: 10.35940/ijrte.B2809.078219
Journal Website: www.ijrte.org

Published By:
Blue Eyes Intelligence Engineering
& Sciences Publication

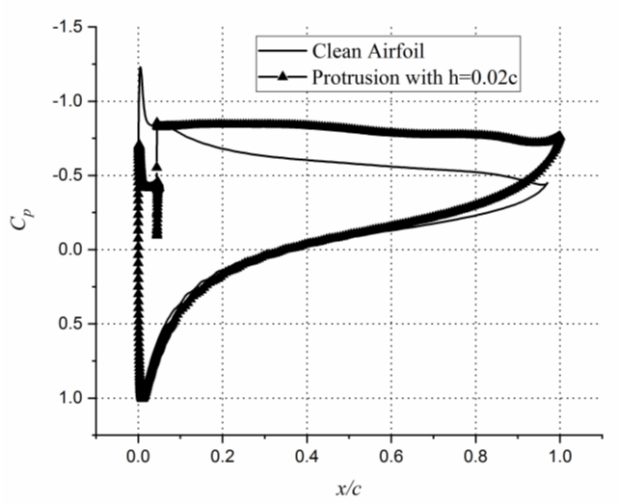

(a)Pressure coefficient at lower lift

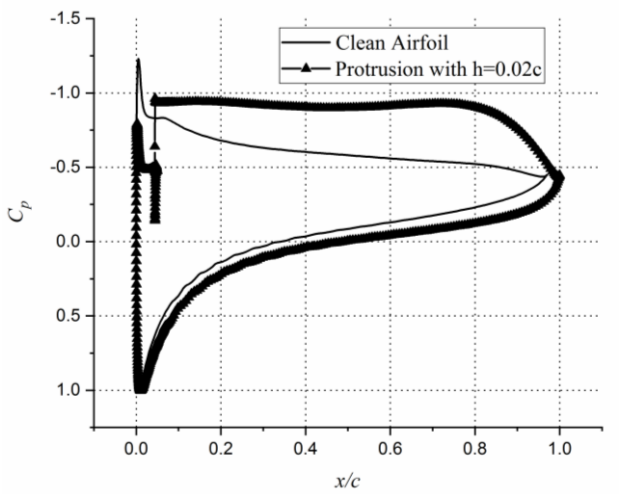

(b) Pressure coefficient at higher lift

(c) Fig. 8: Pressure coefficient over an airfoil with protrusion h=0.02c at 140

Fig.8 explains about the coefficient of pressure distribution around an airfoil when the lift coefficient value is small and high. From the fig.8 (a), it was observed there is a drop in the pressure coefficient value ahead of the protrusion. Whereas at the aft of the protrusion there is a formation of two vortices is present, one of the vortex is about to shed from the surface of the airfoil from the trailing edge due to this there is reduction in the pressure coefficient is detected close to the trailing edge of the airfoil. This the reason to show the lift coefficient value is less even though it is more compared to the clean configuration. In Fig.8 (b), it can be see there is more suction pressure over an airfoil due to strength of the primary vortex. After the vortex sheds from the surface the airfoil the primary vortex forms on the entire surface of the airfoil and gains the strength to increase the lift coefficient value. These shedding vortices results in the minimum and maximum lift coefficient values. From the results, can summarize the effect of protrusion with appropriate height can improve the aerodynamics characteristics of the wings or turbines, so these outcomes of the research work can play a crucial part in the design of low Reynolds number vehicles, bio inspired wing designs and the energy harvesters**.**

IV. CONCLUSION

In this research paper, numerical investigation carried out an airfoil with protrusion at the Reynolds number 100000. The location of the protrusion at 0.05c with three different heights of protrusion 0.005c, 0.01c, 0.02c at various angles of attack from 0^0 to 16^0 with 2^0 intervals. From the results it was found protrusion with height of 0.005c is showing the slight drop in lift coefficient compared to the clean airfoil at 4^0 and 6^0. Whereas for h=0.01c, h=0.02c the performance of the protrusion is not efficient. In case of higher angle of there is an improvement in the lift coefficient observed in all heights, but noticeable rise in lift coefficient is appreciated at h=0.02c. The improvement in the lift coefficient at high angle of attack is revealed due to the shedding of the vortices from the surface of the airfoil. These protrusions can place in the wind turbines to enhance the aerodynamics performance and extract the more energy, unmanned aerial vehicles to enhance their performance. Therefore, these outcomes of the research work play a main role while designing the wings for low Reynolds number vehicles and energy harvesters. In future the research work can carried out at lower and higher angle of attacks with different size of protrusions, at various locations, with different shapes and at different Reynolds number.

ACKNOWLEDGMENT

All the required numerical analysis work is done on CFD servers with 8core Xeon processors and 32 GB memory provided by the University of Petroleum and Energy Studies. We would like to thank the University management for providing us the support to complete this research work.

REFERENCES

1. Lissaman, P. B. S., “Low-reynolds-number airfoils,” Ann. Rev. Fluid Mech., 1983, pp. 223–239.
2. Kelly J. Corfeld, Roger C. Strawn, Lyle N. Long, Computational analysis of a prototype Martian Rotorcraft Experiment. 20th AIAA Applied Aerodynamics Conference, 24-26 June 2002.
3. Kinsey, T., and Dumas, G., (2008). Parametric Study of an Oscillating Airfoil in a Power-Extraction Regime. AIAA Journal, 46: 1318–1330.
4. Xiao, Q., and Zhu, Q., (2014). A review on flow energy harvesters based on flapping foils. Journal of Fluids and Structures, 46: 174–191.
5. Cherubini, A., Papini, A., Vertechy, R., and Fontana, M., (2015). Airborne Wind Energy Systems: A review of the technologies. Renewable and Sustainable Energy Reviews, 51: 1461–1476.
6. Argatov, I., Rautakorpi, P., and Silvennoinen, R., (2009). Estimation of the mechanical energy output of the kite wind generator. Renewable Energy, 34: 1525–1532.
7. Wang, D. A., Chiu, C. Y., and Pham, H. T., (2012). Electromagnetic energy harvesting from vibrations induced by Kármán vortex street. Mechatronics, 22: 746–756.
8. Rostami, A. B., and Armandei, M., (2017). Renewable energy harvesting by vortex-induced motions: Review and benchmarking of technologies. Renewable and Sustainable Energy Reviews, 70: 193–214.
9. Peng, Z., and Zhu, Q., (2009). Energy harvesting through flow-induced oscillations of a foil. Physics of Fluids, 21: 1–9.
10. Kumar, S. K., Bose, C., Ali, S. F., Sarkar, S., and Gupta, S., (2017). Investigations on a vortex induced vibration based energy harvester. Applied Physics Letters, 111: 243903(1-5).
11. Carmichael, B. H., (1982). Low Reynolds Number Airfoil Survey. 1: NASA Report No. 165803.
12. Lin, J. C. M., and Pauley, L. L., (1996). “Low-Reynolds-Number Separation on an Airfoil,” AIAA Journal, 34.

13. Juanmian, L., Feng, G., and Can, H., (2013). Numerical study of separation on the trailing edge of a symmetrical airfoil at a low Reynolds number. Chinese Journal of Aeronautics, 26: 918–925.
14. Yarusevych, S., Sullivan, P. E., Kawall, J. G., (2006). Coherent structures in an airfoil boundary layer and wake at low Reynolds numbers. Physics of Fluids. 44101.
15. Winslow, J., Otsuka, H., Govindarajan, B., and Chopra, I., (2017). Basic Understanding of Airfoil Characteristics at Low Reynolds Numbers. 7th AHS Technical Meeting on VTOL Unmanned Aircraft Systems.
16. Zhang, Y., Igarashi, T., and Hu, H., (2011). Experimental Investigations on the Performance Degradation of a Low-Reynolds-Number Airfoil with distributed leading edge roughness. 49th AIAA Aerospace Sciences Meeting including the New Horizons Forum and Aerospace Exposition, 1–18.
17. Mirzaei, M., Ardekani, M. A., and Doosttalab, M., (2009). Numerical and experimental study of flow field characteristics of an iced airfoil. Aerospace Science and Technology, 13: 267–276.
18. Hansen, K. L., Kelso, R. M., and Dally, B. B., (2011). Performance Variations of Leading-Edge Tubercles for Distinct Airfoil Profiles. AIAA Journal, 49: 185–194.
19. Peristy, L. H., Perez, R. E., Asghar, A., and Allan, W. D. E., (2016). Reynolds Number Effect of Leading Edge Tubercles on Airfoil Aerodynamics" AIAA Aviation.
20. Menter, F. R., Langtry, R. B., Likki, S. R., Suzen, Y. B., Huang, P. G., and Völker, S., (2004). A Correlation-Based Transition Model Using Local Variables: Part I — Model Formulation. Turbo Expo 2004, 4: 57–67.
21. Menter, F. R., (1994). Two-equation eddy-viscosity turbulence models for engineering applications. AIAA Journal, 32: 1598–1605.
22. Ohtake, T., Nakae, Y., and Motohashi, T., "Nonlinearity of the Aerodynamic characteristics of NACA0012 Aerofoil at Low Reynolds Number," Journal of the Japan Society for Aeronautical and Space Sciences, Vol. 55, 2007, pp.439-445.
23. Joshua N. N. Counsil and Kiari Goni Boulama, "Low-Reynolds-Number Aerodynamic Performances of the NACA0012 and Selig-Donovan 7003 Airfoils," Journal of Aircraft, vol. 50, 2013.

AUTHORS PROFILE

Aslesha Bodavula is pursuing her PhD in Aerospace Engineering, UPES, Dehradun. She is specialized in Computational Fluid Dynamics in Masters and Aeronautical Engineering in Bachelors**.** She has published in one International Journal (Indexed in Sci Indexing) and 2 Conference Papers (one International and one National). Her research area is Aerodynamics of low Reynolds number flows, Computational Fluid Dynamics and Numerical Simulations.

Prof. Dr. Ugur Guven is a Senior Professor in Department of Aerospace Engineering UPES, Dehradun. He is an Aerospace Engineer and a Nuclear Engineer. Areas of interest are Nuclear Space Propulsion along with Utilization of CFD in analyzing Nuclear Reactors and Analysis of Energy Systems. He is also interested in Generation IV Reactors, and improvements in energy production. He has worked as part of Research project to NATO on International Radiological Threat Reduction Program. Dr Ugur Guven has published many papers in the field of Interstellar Space Exploration, Nuclear Propulsion Techniques, Mining on the Moon, Fusion Technologies, advanced nuclear methods. He has written over 50 papers, 30 opinion articles and 4 books on future of space technology and nuclear technology. Dr. Guven has taught wide range of courses and he is coordinator in an Experimental Nanosatellite project.
Specialties: Academician, Researcher, Professional Engineer, Nuclear Engineering, Aerospace Engineering, Computational Fluid Dynamics, Teaching at Different IQ and EQ Levels, Technical Project Management, R&D, Engineering Consulting, Career Coaching for Graduating Students

Dr. Rajesh Yadav is an Assistant Professor in Department of Aerospace Engineering, UPES, Dehradun. He has done his Bachelors in Aeronautical Engineering from The Aeronautical Society of India. He ranked in GATE 2006 AIR-8, 2009 AIR-12. His area of Specialization is Aerodynamics, Compressible Flows, Hypersonic Flows, Aerothermodynamics, Computational Fluid Dynamics, and Numerical Simulations

He has 7 SCI Indexed Journal Publications, 8 International Conference Papers, and 4 National Conference Papers. He edited 2 Books. He has 2 Scopus indexed book chapters.
He has life Membership in the Aeronautical Society of India and the Combustion Institute-India